The EMBO Journal Vol. 20 No. 21 pp. 5898–5907, 2001

Immunoproteasome assembly and antigen presentation in mice lacking both PA28α and PA28β

Shigeo Murata, Heiichiro Udono[1], Nobuyuki Tanahashi, Nobuyuki Hamada[2], Ken Watanabe[2], Kei Adachi[2], Taketoshi Yamano[1], Katsuyuki Yui[1], Nobuyuki Kobayashi[2], Masanori Kasahara[3], Keiji Tanaka and Tomoki Chiba[4]

Department of Molecular Oncology, Tokyo Metropolitan Institute of Medical Science, and CREST, Japan Science and Technology Corporation, Tokyo 113-8613, [1]Department of Medical Zoology and Immunology, School of Medicine and [2]Laboratory of Molecular Biology of Diseases, School of Pharmaceutical Sciences, Nagasaki University, Nagasaki 852-8521 and [3]Department of Biosystems Science, School of Advanced Sciences, Graduate University for Advanced Studies, Hayama 240-0193, Japan

[4]Corresponding author
e-mail: tchiba@rinshoken.or.jp

Two members of the proteasome activator, PA28α and PA28β, form a heteropolymer that binds to both ends of the 20S proteasome. Evidence *in vitro* indicates that this interferon-γ (IFN-γ)-inducible heteropolymer is involved in the processing of intracellular antigens, but its functions *in vivo* remain elusive. To investigate the role of PA28α/β *in vivo*, we generated mice deficient in both PA28α and PA28β genes. The ATP-dependent proteolytic activities were decreased in PA28α$^{-/-}$/β$^{-/-}$ cells, suggesting that 'hybrid proteasomes' are involved in protein degradation. Treatment of PA28α$^{-/-}$/β$^{-/-}$ cells with IFN-γ resulted in sufficient induction of the 'immunoproteasome'. Moreover, splenocytes from PA28α$^{-/-}$/β$^{-/-}$ mice displayed no apparent defects in processing of ovalbumin. These results are in marked contrast to the previous finding that immunoproteasome assembly and immune responses were impaired in PA28β$^{-/-}$ mice. PA28α$^{-/-}$/β$^{-/-}$ mice also showed apparently normal immune responses against infection with influenza A virus. However, they almost completely lost the ability to process a melanoma antigen TRP2-derived peptide. Hence, PA28α/β is not a prerequisite for antigen presentation in general, but plays an essential role for the processing of certain antigens.

Keywords: antigen processing/gene targeting/immunoproteasome/PA28α/PA28β

Introduction

The proteasome is a large multicatalytic cytoplasmic and nuclear protease complex that is responsible for the majority of non-lysosomal protein degradation within eukaryotic cells (reviewed in Coux *et al*., 1996; Voges *et al*., 1999). Its catalytically active core particle, the 20S proteasome, is a barrel-shaped complex made of two outer α-rings and two inner β-rings. The α- and β-rings are each made up of seven structurally similar α- and β-subunits, respectively. The proteolytic activity is exerted by three of the β-subunits, namely β1 (also called Y in vertebrates), β2 (Z) and β5 (X) (reviewed in Bochtler *et al*., 1999). Tertiary structural analysis indicates that the center of the α-ring is almost closed, thus preventing penetration of substrates into the interior of the β-ring on which the proteolytically active sites are located (Bochtler *et al*., 1999; Voges *et al*., 1999). Because of this structural feature, the 20S proteasome exists in a latent form in cells. The latent proteasome is activated by association with two regulatory complexes, known as PA700 and PA28, which bind to the α-ring of the 20S proteasome.

PA700 or the 19S complex is a 700 kDa protein complex composed of ~20 subunits with sizes of 25–110 kDa (reviewed in Tanaka, 1998), which are organized into two distinguishable subcomplexes: the base and the lid (Glickman *et al*., 1998). PA700 can associate with the 20S proteasome in an ATP-dependent manner, producing the 26S proteasome, the ATP-dependent protease complex with a molecular mass of ~2.5 MDa. The 26S proteasome is responsible for the degradation of a wide variety of cellular proteins tagged with a polyubiquitin chain, which serves as a degradation signal (reviewed in Hershko and Ciechanover, 1998).

PA28 or the 11S regulator (REG) was identified as another activator of the latent 20S proteasome (Dubiel *et al*., 1992; Ma *et al*., 1992). PA28 is composed of two subunits, named PA28α and PA28β, which share ~50% amino acid identity. These subunits assemble into a heteroheptameric ring with nearly equal stoichiometric amounts of PA28α and PA28β (reviewed in Rechsteiner *et al*., 2000). Association of PA28 with the 20S proteasome does not require energy and greatly stimulates multiple peptidase activities of the 20S proteasome *in vitro*. However, it fails to enhance the hydrolysis of large protein substrates with native or denatured structures, even when they are ubiquitylated. Later, another PA28 protein, termed PA28γ, was found to form homopolymers and activate peptidase activities of the 20S proteasome (Tanahashi *et al*., 1997).

The major role of the proteasome is the degradation of intracellular proteins, a task that is essential for cell viability. Proteasomes are also the central enzymes responsible for the generation of major histocompatibility complex (MHC) class I-binding peptides or ligands (reviewed in Rock and Goldberg, 1999; Kloetzel, 2001). This idea is supported by the observation that specific inhibition of proteasomes by lactacystin or peptide aldehydes impairs the presentation of peptides by MHC class I molecules (Rock *et al*., 1994). Recent work indicates that peptides arising from proteasomal degradation of defective ribosomal products constitute a major

source of MHC class I-binding peptides (Reits *et al*., 2000; Schubert *et al*., 2000).

In jawed vertebrates, when cells are exposed to interferon-γ (IFN-γ), the three catalytic subunits of the standard 20S proteasome, X (β5), Y (β1) and Z (β2), are replaced by their IFN-γ-inducible counterparts, LMP7 (β5i), LMP2 (β1i) and MECL1 (β2i), respectively, leading to the formation of the 'immunoproteasome' (reviewed in Tanaka and Kasahara, 1998; Fruh and Yang, 1999). Accumulated evidence indicates that the cleavage specificities of the immunoproteasome are different from those of the standard proteasome and that the immunoproteasome produces peptides capable of binding to MHC class I molecules more efficiently. Consistent with this, the ability to process certain viral antigens was impaired in mice lacking LMP7 or LMP2 (Fehling *et al*., 1994; Van Kaer *et al*., 1994).

Like LMP2, LMP7 and MECL1, expression of PA28α and PA28β is increased markedly upon stimulation with IFN-γ, suggesting their involvement in antigen processing. Indeed, *in vitro* studies showed that the PA28α/β complex facilitates dual cleavage excision of MHC class I ligands from polypeptide precursors by the 20S proteasome (Dick *et al*., 1996). Furthermore, overexpression of the PA28α subunit in cells was shown to enhance the antigen presentation of some viral epitopes (Groettrup *et al*., 1996). More recently, mice deficient in the *PA28β* gene were found to develop marked defects in antigen presentation (Preckel *et al*., 1999). Interestingly, immunoproteasome assembly was impaired in the spleen cells of these mice, indicating that PA28 is required for the formation of the immunoproteasome. In the PA28β$^{-/-}$ mice, splenocytes lacked not only PA28β proteins, but also nearly all PA28α proteins, suggesting that PA28α and PA28β always function as a heterocomplex *in vivo*. This is in apparent conflict with the observation that PA28α forms a stable homoheptamer and functions as a competent proteasome activator *in vitro* (Rechsteiner *et al*., 2000).

To assess the precise role of the PA28α/β complex *in vivo*, we generated mice lacking both *PA28α* (*Psme1*) and *PA28β* (*Psme2*) genes. These mice showed decreased ATP-dependent proteolytic activities, indicating that 'hybrid proteasomes' that contain both PA28 and PA700 (Hendil *et al*., 1998; Tanahashi *et al*., 2000) are involved in protein degradation in the cells. However, they showed defects neither in immunoproteasome assembly nor in the ability to process ovalbumin (OVA) *in vitro*. Furthermore, these mice were capable of mounting normal cytotoxic T-lymphocyte (CTL) responses against influenza A virus infection. Thus, our results are in marked contrast to the observations made in the PA28β$^{-/-}$ mice, which suggested that PA28α/β is essential for immunoproteasome assembly and antigen presentation (Preckel *et al*., 1999). Interestingly, we found that processing of certain melanoma tumor antigens was greatly impaired in PA28α/β-deficient mice. These data indicate that the PA28α/β complex is not a prerequisite for antigen processing in general, but is required for processing of certain antigens. We also found, using knockout mice lacking all three *PA28* genes, that the loss of PA28γ, the third member of the PA28 family, does not affect antigen presentation.

Results

Generation of PA28α/β-deficient mice

The genes for PA28α and PA28β are tightly linked and only 6 kb apart (Kohda *et al*., 1998). Hence, both genes can be disrupted by a single homologous recombination event. We selected embryonic stem (ES) cells, in which the homologous recombination had taken place, using the method of positive and negative selection. Figure 1A shows the structure of the targeting vector. Homologous recombination with the endogenous *PA28α* and *PA28β* genes will delete a 2.1 kb *Ssp*I–*Xba*I fragment of the *PA28α* gene spanning from part of the first intron to part of the last exon, and replace an internal 3.1 kb *Apa*I–*Cla*I fragment of the *PA28β* gene containing part of the first intron to part of the last exon with a neo gene cassette. The space between the two *PA28* genes contains a ubiquitously expressed gene designated *Cgi112* (Yawata *et al*., 2001). The homologous recombination does not destroy the *Cgi112* gene.

The linearized targeting construct was transfected into TT2 ES cells. Analysis of 159 independent G418-resistant clones by PCR and consecutive Southern blot analysis identified three ES clones with a targeted mutation. Two of them were injected into ICR blastocysts, which both developed into chimeric mice that transmitted the mutated *PA28α/β* allele through the germline.

Crosses of the PA28α$^{+/-}$/β$^{+/-}$ mice resulted in progeny with the expected Mendelian frequencies. Figure 1B shows a representative Southern blot analysis using genomic DNA isolated from wild-type and mutant mice. Mice homozygous for the *PA28α/β* mutation bred well, were apparently healthy, had no gross anatomical abnormalities and lived to at least 1 year of age. Northern blot analysis of IFN-γ-untreated and -treated mouse embryonic fibroblasts (MEFs) confirmed that the mutant mice expressed the messages of neither the *PA28α* nor the *PA28β* gene (Figure 1C). Northern blot analysis of the brain, liver, spleen, small intestine and skeletal muscle of the mutant mice also confirmed the complete absence of the PA28α and PA28β mRNA (data not shown). Western blot analysis likewise showed the loss of the PA28α and PA28β proteins even after IFN-γ stimulation (Figure 1D). It has been reported that there are at least two functional *PA28α* genes (Preckel *et al*., 1999) and two functional *PA28β* genes (Zaiss and Kloetzel, 1999). Our results, however, indicate strongly that the mouse genome contains only one copy each of the functional gene for PA28α and PA28β.

PA28α/β-deficient mice do not display any obvious abnormalities in subcellular distribution or expression levels of proteasomal components

The PA28 family has three members. While PA28α/β exists predominantly in the cytosol and on microsomes, the third member of the family, PA28γ, exists mainly in the nucleus (Wojcik *et al*., 1998; Brooks *et al*., 2000). We first examined whether the depletion of PA28α/β has any effect on the expression level and subcellular distribution of PA28γ. Figure 1D shows that the expression level of the PA28γ protein in MEFs is almost identical between the mutant and wild-type mice. To examine whether the absence of PA28α/β alters the subcellular distribution of PA28γ, we separated cytosol and membrane fractions from

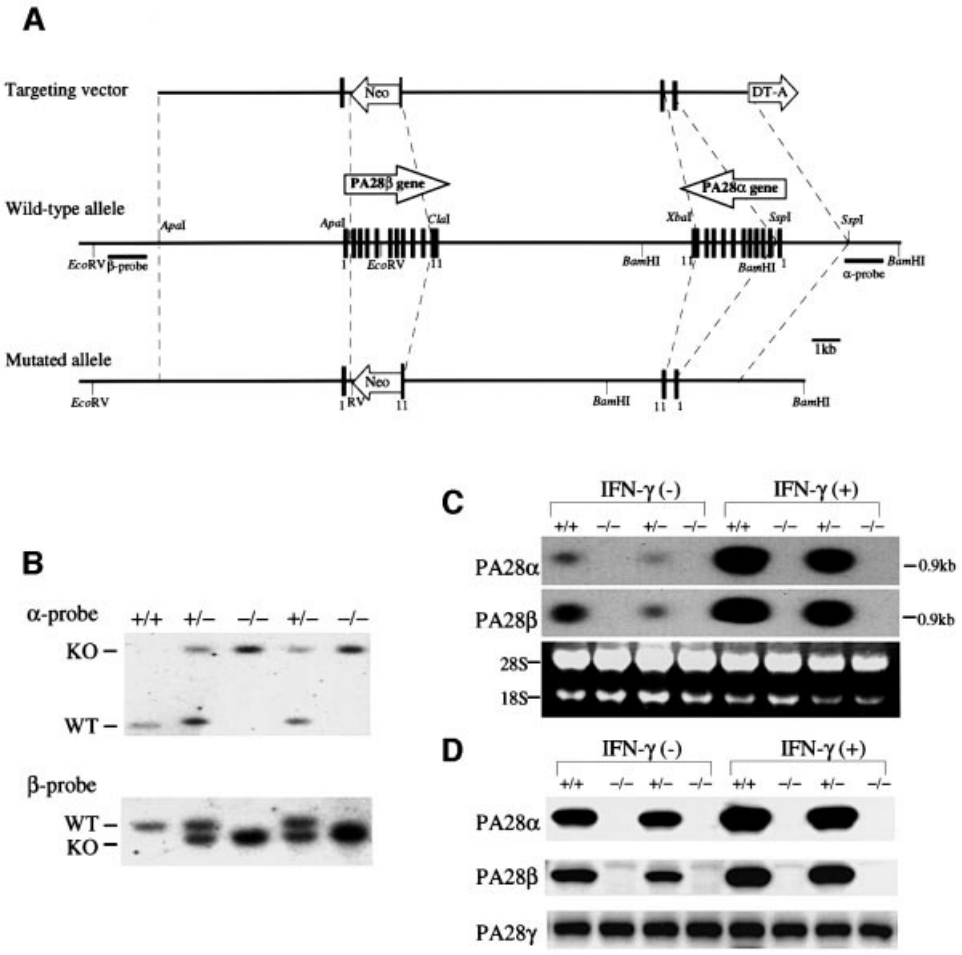

Fig. 1. Disruption of the *PA28α* and *PA28β* genes by homologous recombination. (**A**) Structure of the targeting vector, the wild-type *PA28α/β* genes and the mutated *PA28α/β* genes following homologous recombination. Relevant restriction enzyme sites are indicated. Exons are depicted as closed boxes. The first and the last exons of the *PA28α/β* genes are numbered 1 and 11, respectively. The probes used for Southern blot analysis are shown as α- and β-probes. (**B**) Southern blot analysis. Genomic DNA extracted from mouse tails was digested with *Bam*HI or *Eco*RV, blotted, and hybridized with the α- or the β-probe shown in (A), respectively. The wild-type allele (WT) gave a 2.5 kb fragment for the α-probe and a 9.0 kb fragment for the β-probe, while the mutant allele (KO) gave a 4.8 kb fragment for the α-probe and a 7.5 kb fragment for the β-probe. (**C**) Northern blot analysis. Total RNAs isolated from MEFs cultured with or without IFN-γ for 36 h were hybridized with the full-length mouse PA28α or PA28β cDNA probe. 28S and 18S rRNAs were stained with ethidium bromide to monitor the integrity of RNA. (**D**) Western blot analysis. Protein lysates from MEFs cultured with or without IFN-γ for 72 h were used to examine the expression of PA28α, β and γ.

mouse tissues and performed western blot analysis (Figure 2). PA28γ, believed to be a nuclear protein based on immunocytochemical analysis, was also detectable in both fractions, as previously reported (Wojcik, 1999). The expression level of PA28γ did not show any increase in the cytosolic or membrane fraction of PA28α$^{-/-}$/β$^{-/-}$ mice, suggesting that PA28γ does not compensate for the loss of PA28α/β. To confirm these results, we also performed immunocytochemical analysis of MEFs derived from the PA28α$^{-/-}$/β$^{-/-}$ and wild-type mice. This analysis showed that the staining pattern of PA28γ does not change in the absence of PA28α/β (data not shown).

We then examined whether the deficiency of PA28α/β alters the expression levels and distribution patterns of other proteasomal components (Figure 2). LMP2 is the component of the immunoproteasome that replaces Y, and X is the subunit of the standard proteasome that is replaced by LMP7 upon IFN-γ stimulation. These subunits of the 20S proteasome showed no change in expression levels or their relative abundance in the cytosolic/membrane fractions. Similarly, Mss1, the component of PA700, showed no alteration in its expression level or distribution pattern. These results indicate that PA28α/β influences neither the intracellular localization nor the expression level of other proteasomal components.

In the brain of wild-type mice, PA28α was more abundant than PA28β, while their expression levels were nearly equal in spleen and liver (Figure 2), as we recently observed in the rat (Noda *et al*., 2000).

ATP-dependent proteolysis is attenuated in PA28α/β-deficient mice

We recently demonstrated the existence of the 'hybrid proteasome', the 20S proteasome that binds PA28 on one side and PA700 on the other side (Hendil *et al*., 1998; Tanahashi *et al*., 2000), and showed that this type of proteasome, the formation of which is up-regulated by IFN-γ stimulation, participates in ATP-dependent protein degradation (Tanahashi *et al*., 2000). Naturally, PA28α$^{-/-}$/β$^{-/-}$ mice should lack hybrid proteasomes.

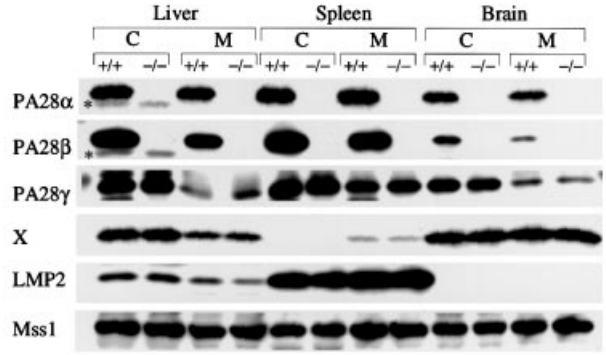

Fig. 2. Expression of proteasomal components in the cytosolic and membrane fractions of various tissues from wild-type and PA28α$^{-/-}$/β$^{-/-}$ mice. Cytosolic (C) and membrane (M) proteins were isolated from the liver, spleen and brain of wild-type and knockout mice as described in Materials and methods. The ratios of protein content in cytosolic and membrane fractions were 2.4:1 in the liver, 5.6:1 in the spleen and 3.0:1 in the brain. Samples (10 μg of proteins) were analyzed by SDS–PAGE and western blotting using antibodies against PA28α, PA28β, PA28γ, X, LMP2 and Mss1. Asterisks indicate artifact bands produced by the PA28α and PA28β antibodies.

To verify the role of the hybrid proteasome in protein degradation, we examined whether the ability to degrade ornithine decarboxylase (ODC), which is degraded by the 26S proteasome without ubiquitylation (Murakami *et al*., 1992, 1999), was altered in the PA28α$^{-/-}$/β$^{-/-}$ mice. The crude cytosolic extracts of PA28α$^{-/-}$/β$^{-/-}$ MEFs showed decreased ODC degradation activities compared with those in wild-type MEFs, and this difference became more pronounced when the MEFs were treated with IFN-γ (Figure 3A). Glycerol density gradient centrifugation analysis of the extracts revealed that ODC degradation activities around the 26S proteasome fractions (fraction 18 and its adjacent fractions) were decreased in the mutant extracts, particularly in those extracts obtained from IFN-γ-treated PA28α$^{-/-}$/β$^{-/-}$ MEFs (Figure 3B). In contrast, the peptidase specificities and activities of the 20S proteasome fractions (fraction 14 and its adjacent fractions) as well as those of the 26S proteasome fractions showed little, if any, alteration in PA28α$^{-/-}$/β$^{-/-}$ MEFs, regardless of whether MEFs were treated with IFN-γ or not (Figure 3C). Note that the fractions containing PA28α (fractions 14–16) exhibited higher *t*-butyloxycarbonyl-Leu-Arg-Arg-AMC (Boc-LRR-AMC) hydrolysis activities in wild-type than in PA28α/β-deficient cells when cells were treated with IFN-γ. To confirm these results, we performed the same experiments using splenic extracts instead of MEFs. These experiments yielded results similar to those shown in Figure 3A–C (data not shown). Thus, we conclude that, presumably as a component of the hybrid proteasome, PA28α/β promotes degradation of native proteins without affecting the catalytic activities of the core 20S proteasome, and that this enhancing effect is up-regulated by IFN-γ.

Immunoproteasome assembly is not impaired in PA28α/β-deficient mice

Preckel *et al*. (1999) reported that PA28β-deficient mice had impaired CTL responses and lacked immunoproteasomes. In sharp contrast to their results, we found that PA28α$^{-/-}$/β$^{-/-}$ mice express normal levels of the immunoproteasomal component LMP2 (Figure 2). Glycerol density gradient centrifugation analysis revealed that IFN-γ-treated MEFs (Figure 3B) and splenocytes (data not shown) derived from the PA28α$^{-/-}$/β$^{-/-}$ mice contained functional immunoproteasomes at a level comparable with that in wild-type MEFs and splenocytes. We also examined whether the initial assembly of immunoproteasomes was impaired in the mutant extracts (Figure 3D). MEFs did not express LMP2 without IFN-γ treatment. The LMP2 polypeptide became detectable after 12 h upon stimulation with IFN-γ, and its expression level increased up to 48 h. On the contrary, the expression level of the X subunit, one of the subunits of the standard proteasome, decreased as the amount of LMP2 increased. Neither the induction rate of LMP2 nor the disappearance rate of X showed any obvious difference between the wild-type and PA28α$^{-/-}$/β$^{-/-}$ MEFs. Two-dimensional PAGE of MEFs treated with IFN-γ also revealed normal incorporation of immunoproteasomal components into the 20S proteasome in PA28α/β-deficient cells (Figure 3E). These results clearly show that immunoproteasome assembly is not impaired in PA28α/β-deficient mice.

Efficient presentation of OVA antigen and normal immune responses to influenza A virus infection, but impaired presentation of TRP2 antigen in PA28α/β-deficient mice

Several lines of evidence indicate that PA28α/β enhances generation of MHC class I-binding peptides by the proteasome and is involved in the immune surveillance of foreign invaders such as viruses (Tanaka and Kasahara, 1998; Stoltze *et al*., 2000). To examine whether the absence of PA28α/β impairs MHC class I-restricted antigen presentation, we first examined the cell surface expression pattern of MHC class I molecules by fluorescence-activated cell sorting (FACS) analysis. The mean fluorescence intensities for the H2-K^b molecule showed no difference between the mutant and wild-type cells (data not shown), indicating that surface expression levels of class I molecules are not reduced by the absence of PA28α/β. The mutant mice contained normal numbers of CD4-positive T cells and CD8-positive T cells in spleen and thymus, and the number of splenic B cells in the mutant mice was normal (data not shown).

The apparent absence of gross immunological abnormalities in the PA28α$^{-/-}$/β$^{-/-}$ mice prompted us to examine the ability of these mice to generate specific CTL epitopes. Preckel *et al*. (1999) reported that their PA28β-deficient mice were unable to generate the OVA$_{257–264}$ epitope (amino acids 257–264 of the OVA sequence). We therefore tested the capacity of LPS blasts made from wild-type and PA28α$^{-/-}$/β$^{-/-}$ splenocytes to process OVA for presentation to an H2-K^b-restricted OVA$_{257–264}$-specific CTL clone. In sharp contrast to the results of Preckel *et al*., we found that CTL responses in OVA-loaded cells were not impaired in PA28α$^{-/-}$/β$^{-/-}$ splenocytes even when the loading dose of OVA was suboptimal (Figure 4A).

CTLs play an important role in protection against and recovery from acute viral infections. To examine whether the absence of PA28α/β impairs *in vivo* immune responses, we infected wild-type and PA28α$^{-/-}$/β$^{-/-}$ mice

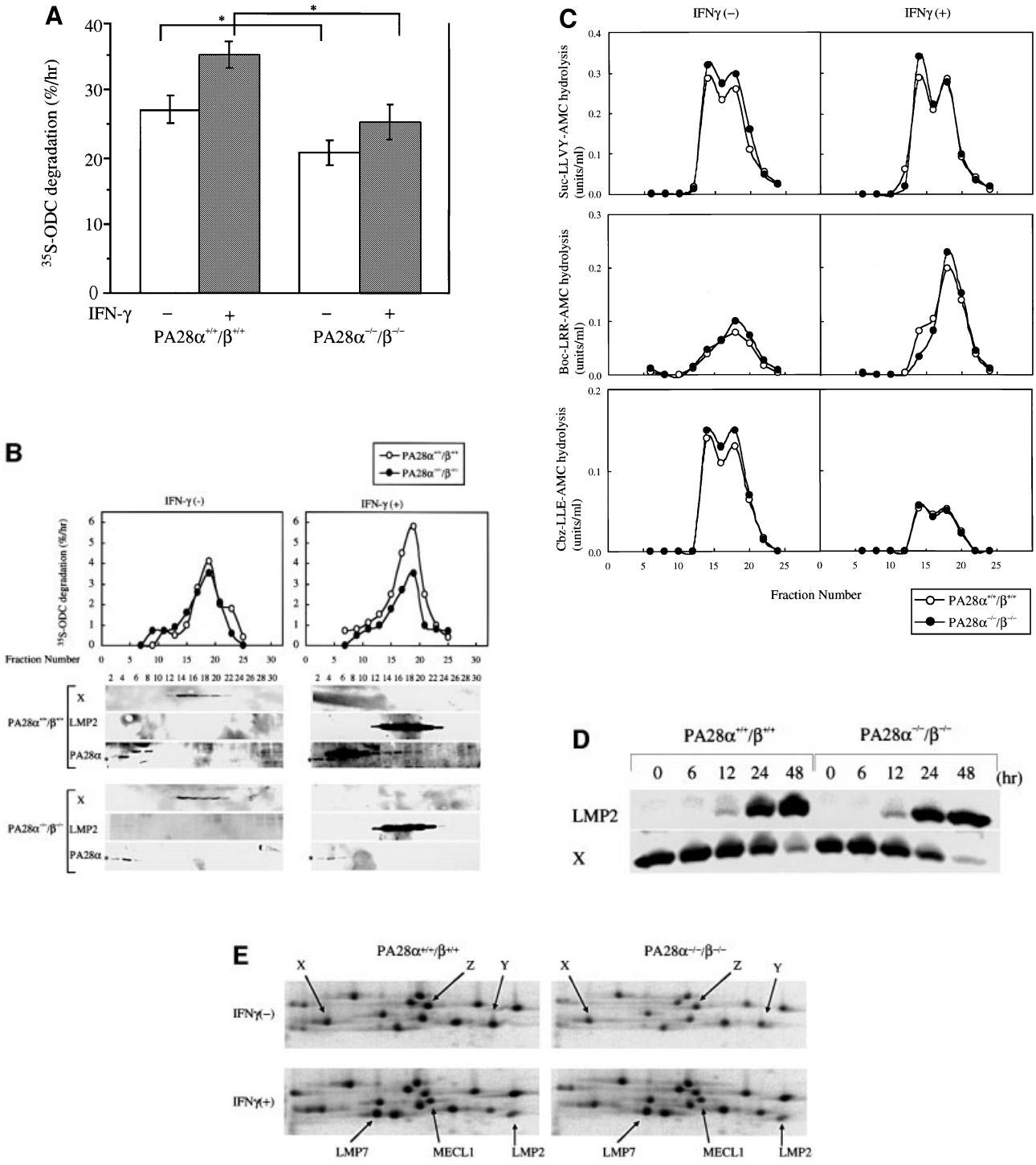

Fig. 3. ATP-dependent protein degradation activity, peptide hydrolysis activities and immunoproteasome formation in wild-type and PA28α$^{-/-}$/β$^{-/-}$ cells. (**A**) ATP- and AZ-dependent degradation of [^{35}S]ODC was assayed using crude extracts from wild-type and knockout MEFs cultured with (filled bars) or without (open bars) IFN-γ for 72 h. The results are the mean of determinations performed in triplicate. Error bars represent one standard deviation on each side of the mean. There are statistically significant differences between wild-type and PA28α$^{-/-}$/β$^{-/-}$ cells (P <0.01, shown as asterisks). The experiment was repeated three times and consistently yielded statistically significant differences between wild-type and knockout MEFs (data not shown). (**B**) Sedimentation velocity analysis. Samples (2 mg of proteins) from wild-type (open circles) and knockout (filled circles) MEFs were fractionated by glycerol density gradient centrifugation (10–40% glycerol from fraction 1 to fraction 30). Aliquots (20 µl) of individual fractions were used for assay of [^{35}S]ODC degradation activities. Western blot analysis of each fraction was performed using antibodies against X, LMP2 and PA28α. Asterisks indicate artifact bands. Numbers correspond to fraction numbers in the upper and lower panels. (**C**) Peptide hydrolysis activities. Aliquots of individual fractions prepared in (B) were subjected to peptide hydrolysis assays using three kinds of substrates. Suc-LLVY-AMC and Cbz-LLE-AMC were hydrolyzed in the presence of 0.05% SDS, whereas Boc-LRR-AMC was hydrolyzed without SDS. Open circles, wild-type; filled circles, knockout. (**D**) Initial assembly of immunoproteasomes. MEFs were cultured in the presence of IFN-γ. After the indicated times (hours), MEFs were harvested for western blot analysis with anti-LMP2 and anti-X antibodies. (**E**) Two-dimensional gel electrophoresis. MEFs were cultured in the presence or absence of IFN-γ for 48 h, and then metabolically labeled for 4 h followed by a 16 h chase. Cell lysates were immunoprecipitated with anti-20S proteasome antibodies and subjected to isoelectric focusing followed by SDS–PAGE.

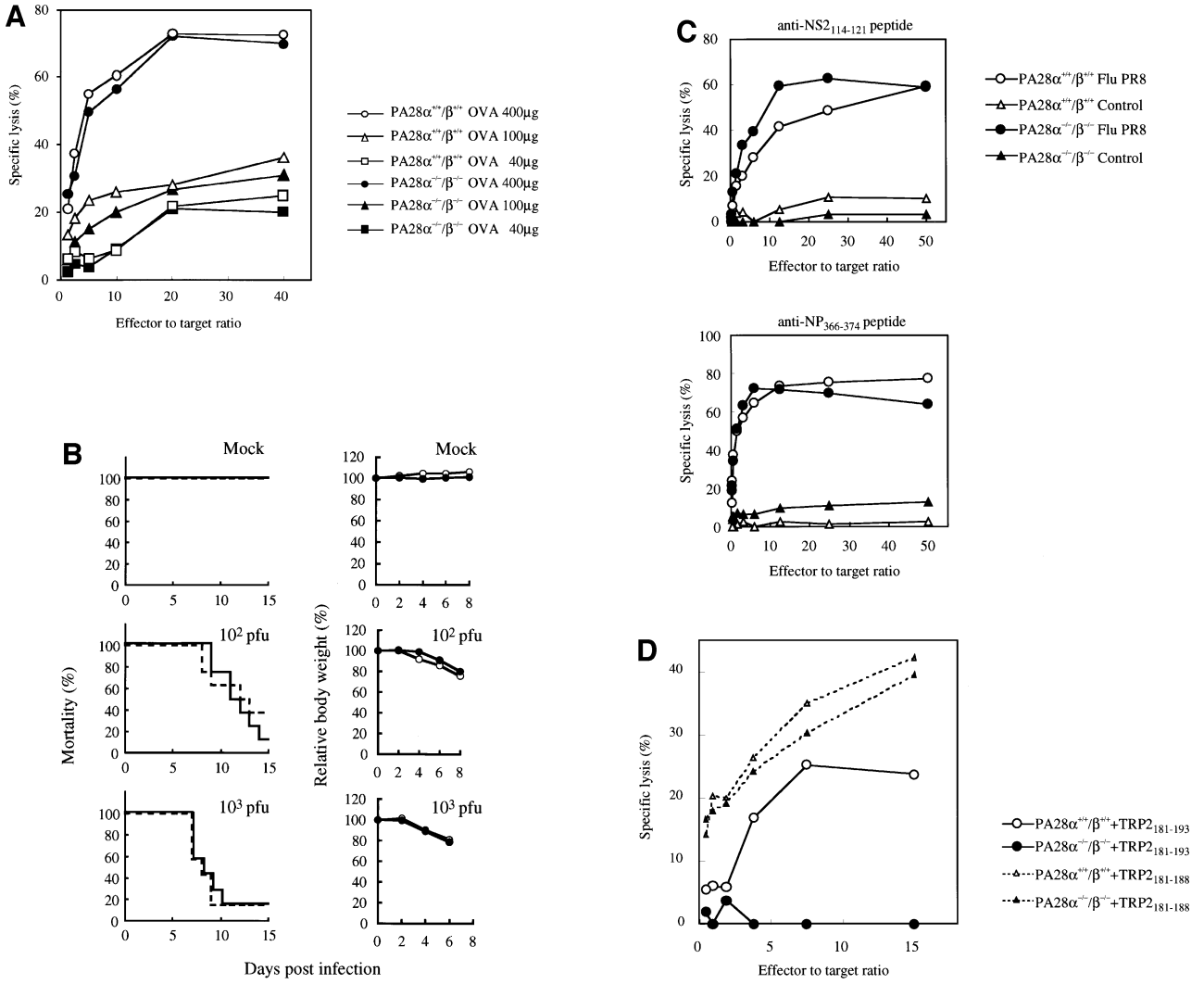

Fig. 4. Role of PA28α/β in antigen processing and immune responses against viral infection. (**A**) Presentation of the $OVA_{257–264}$ epitope. LPS blasts from wild-type (open symbols) and PA28$\alpha^{-/-}/\beta^{-/-}$ (filled symbols) mice were osmotically loaded with the indicated doses of OVA proteins and labeled with ^{51}Cr. The labeled cells were used as target cells for the lysis by $OVA_{257–264}$-specific CTLs. (**B**) Mortality rates and relative body weight loss after infection with the influenza A virus strain PR8. Mice (n = 8 per group) were infected intranasally with the indicated doses of Flu PR8. Mortality rates in wild-type (dashed line) and PA28$\alpha^{-/-}/\beta^{-/-}$ (solid line) mice are shown on the left. Relative body weight loss in wild-type (open circles) and PA28$\alpha^{-/-}/\beta^{-/-}$ (filled circles) mice is shown on the right. Data represent the mean percentage body weight relative to the weight before infection. (**C**) CTL induction after Flu PR8 infection. Two weeks after infection with Flu PR8 (circles), splenocytes from wild-type (open symbols) and PA28$\alpha^{-/-}/\beta^{-/-}$ (filled symbols) mice were isolated, stimulated with synthetic peptide $NS2_{114–121}$ or $NP_{366–374}$ for 6 days, and used as effector cells. ^{51}Cr-labeled EL-4 cells pulsed with $NS2_{114–121}$ or $NP_{366–374}$ were used as target cells. Splenocytes from non-infected mice (triangles) were used as a control. (**D**) Presentation of the $TRP2_{181–188}$ epitope. LPS blasts from wild-type (open symbols) and PA28$\alpha^{-/-}/\beta^{-/-}$ (filled symbols) mice were osmotically loaded with the $TRP2_{181–193}$ peptide (circles) or the $TRP2_{181–188}$ peptide (triangles) and labeled with ^{51}Cr. The labeled cells were used as target cells for the lysis by $TRP2_{181–188}$-specific CTLs.

with the influenza A virus strain PR8 (Flu PR8). Figure 4B shows that the mutant and wild-type mice did not differ significantly in mortality rates or the extent of body weight loss. The Flu PR8-specific CTL activity was determined 2 weeks after infection. PA28$\alpha^{-/-}/\beta^{-/-}$ mice infected with Flu PR8 were capable of generating CTL activities almost identical to those in infected wild-type mice when splenic T cells were assayed on EL-4 cells pulsed with a D^b-restricted $NP_{366–374}$ peptide or a K^b-restricted $NS2_{114–121}$ peptide (Figure 4C). These results demonstrate that the proteasome is capable of producing such peptides in a PA28α/β-independent manner, and that PA28α/β itself has little, if any, influence on the production of these CTL epitopes.

We then tested the ability of the mutant mice to present an epitope derived from a tumor antigen of murine B16 melanoma, tyrosinase-related protein (TRP) 2. The dominant CTL epitope in $H2^b$ mice is $TRP2_{181–188}$ (Bloom *et al.*, 1997). The synthetic peptide $TRP2_{181–193}$, which contains the epitope and five additional amino acids in the C-terminus, was loaded onto LPS blasts prepared from wild-type and PA28$\alpha^{-/-}/\beta^{-/-}$ splenocytes. These peptide-pulsed cells were then used as target cells for lysis by an H2-K^b-restricted $TRP2_{181–188}$-specific CTL clone. As

shown in Figure 4D, the CTL clone efficiently lysed wild-type but not PA28α/β-deficient cells pre-loaded with $TRP2_{181–193}$. Treatment with the proteasome inhibitor lactacystin completely eliminated the ability of wild-type cells to process the $TRP2_{181–193}$ peptide (data not shown), indicating that proteasomal cleavage is required for the generation of the $TRP2_{181–188}$ epitope.

Taken together, these results indicate that PA28α/β is not a prerequisite for antigen processing in general, but is essential for producing certain CTL epitopes.

PA28γ does not affect the presentation of TRP2 and OVA antigens

PA28γ is a third member of the PA28 family with the ability to activate the peptidase activities of the 20S proteasome. Unlike PA28α/β, PA28γ is not induced appreciably upon IFN-γ stimulation. It forms a homopolymer that occurs predominantly in the nucleus and does not associate with PA28α or PA28β. PA28γ-deficient mice showed slight growth retardation (Murata *et al*., 1999), but whether the lack of PA28γ impairs antigen presentation remained unsolved. To address this issue, we examined the ability of $PA28\gamma^{-/-}$ and $PA28\alpha^{-/-}/\beta^{-/-}/\gamma^{-/-}$ LPS blasts to present $OVA_{257–264}$ and $TRP2_{181–188}$ epitopes (Figure 5). Both $PA28\gamma^{-/-}$ and $PA28\alpha^{-/-}/\beta^{-/-}/\gamma^{-/-}$ cells were capable of presenting the OVA epitope with efficiencies comparable to those in their wild-type counterparts (Figure 5A). Unlike $PA28\alpha^{-/-}/\beta^{-/-}$ cells, $PA28\gamma^{-/-}$ cells pre-loaded with $TRP2_{181–193}$ were also lysed efficiently by $TRP2_{181–188}$-specific CTLs (Figure 5B). Thus, so far as the antigens examined are concerned, PA28γ does not appear to play a role in antigen presentation.

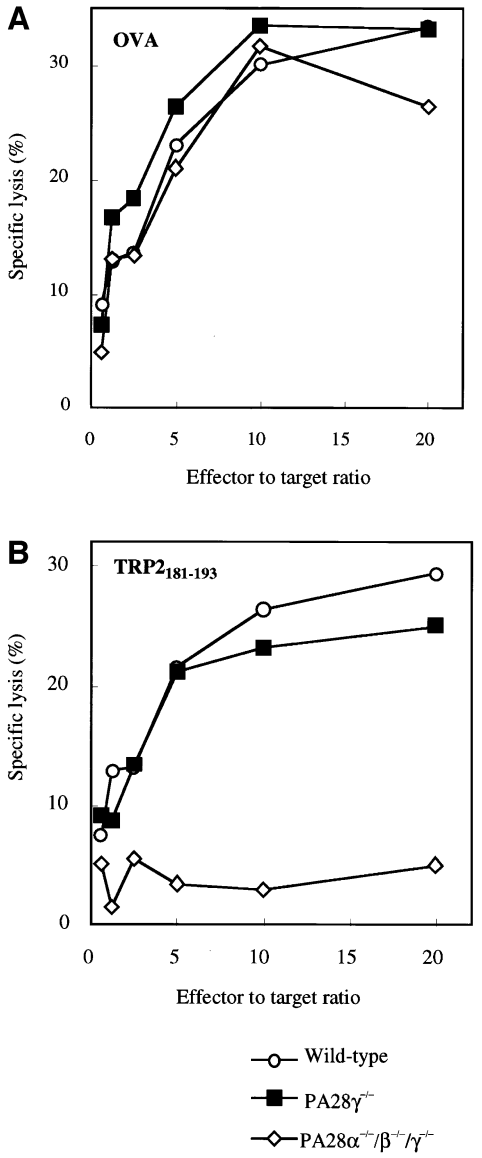

Fig. 5. Role of PA28γ in antigen processing. (**A**) Presentation of the $OVA_{257–264}$ epitope. (**B**) Presentation of the $TRP2_{181–188}$ epitope. Analyses were performed as in Figure 4A and D, respectively. Open circles, wild type; filled squares, $PA28\gamma^{-/-}$; open diamonds, $PA28\alpha^{-/-}/\beta^{-/-}/\gamma^{-/-}$.

Discussion

In the present study, we generated mice lacking both PA28α and PA28β. Previous studies have raised considerable controversy as to the copy number of functional genes coding for PA28α and PA28β. Preckel *et al*. (1999) suggested that there are at least two functional copies of the *PA28α* gene. On the other hand, Zaiss and Kloetzel (1999) described a second, intronless *PA28β* gene driven by the LINE1 promoter, which could encode a polypeptide identical to the known PA28β. However, when we inactivated the previously characterized *PA28α* and *PA28β* genes located in tandem on chromosome 14 (Kohda *et al*., 1998), both the mRNAs and the proteins for PA28α and PA28β disappeared completely in various tissues and cells even after IFN-γ stimulation (Figure 1). These results strongly suggest that the mouse genome, at least that of the C57BL/6 strain used in the present study, contains only one copy each of the functional *PA28α* and *PA28β* genes.

The most significant and somewhat surprising result obtained in this study was that the phenotype of the $PA28\alpha^{-/-}/\beta^{-/-}$ mice differed markedly from that of the $PA28\beta^{-/-}$ mice reported recently (Preckel *et al*., 1999). The $PA28\beta^{-/-}$ mice virtually lacked immunoproteasomes and showed marked defects in CTL responses to lymphocytic choriomeningitis virus. In addition, they were unable to produce the $OVA_{257–264}$ epitope for presentation to CTL. In sharp contrast, we found that immunoproteasome assembly occurs normally in the $PA28\alpha^{-/-}/\beta^{-/-}$ mice (Figures 2 and 3) and that these mice are competent in generating the same $OVA_{257–264}$ epitope (Figure 4A). Furthermore, we found that the $PA28\alpha^{-/-}/\beta^{-/-}$ mice were able to mount apparently normal immune responses against infection with influenza A virus (Figure 4B and C), but lost the ability to generate the $TRP2_{181–188}$ epitope (Figure 4D). Because the $PA28\beta^{-/-}$ mice lacked both immunoproteasomes known to be involved in the processing of endogenous antigens (reviewed in Fruh and Yang, 1999; Niedermann *et al*., 1999; Stoltze *et al*., 2000) and PA28α/β, it was not possible to evaluate directly the role of PA28α/β in antigen processing and presentation. Our present work, which allowed for the assessment of the role of PA28α/β itself, clearly shows that PA28α/β is not required either for immunoproteasome assembly or for

effective presentation of OVA and influenza A virus epitopes, but is essential for processing of some antigens such as TRP2. We suggest that many, if not all, of the defects observed in the PA28β$^{-/-}$ mice occurred as a consequence of the lack of immunoproteasomes. Recent work indicates that overexpression of PA28α/β does not shift proteasome assembly towards the assembly of immunoproteasomes (Schwarz *et al*., 2000b). Thus, neither the absence nor the excess of PA28α/β appears to exert any influence on the assembly of immunoproteasomes.

Why did the phenotypes of the PA28α$^{-/-}$/β$^{-/-}$ and PA28β$^{-/-}$ mice differ so drastically despite the fact that, in addition to PA28β, the latter also lacked nearly all PA28α polypeptides? Although we do not have an answer, one possible explanation is that PA28α homopolymers or monomers, which seem to be unstable *in vivo* in the absence of PA28β (Preckel *et al*., 1999), may interfere with the assembly of the immunoproteasome. One observation consistent with this explanation is that immunoproteasomes or hybrid proteasomes are barely detectable in the mouse or rat brain, where PA28α is much more abundant than PA28β (Figure 2; Noda *et al*., 2000). We speculate that excess PA28α may produce PA28α monomers, PA28α homopolymers or PA28α/β heteropolymers predominantly made up of PA28α, which adversely affect assembly of immunoproteasomes and hybrid proteasomes.

While the role of immunoproteasomes in antigen processing and presentation in the MHC class I pathway is reasonably well established, the role of PA28 is still controversial (Rock and Goldberg, 1999). Some epitopes seem to be presented more efficiently when PA28α/β expression levels are increased, but others are not (Stoltze *et al*., 2000). For example, overexpression of PA28α in cells promoted antigen processing and presentation of influenza and cytomegalovirus proteins (Groettrup *et al*., 1996). On the other hand, Schwarz *et al*. (2000a) showed that overexpression of PA28α/β did not enhance the production of a nucleoprotein epitope of lymphocytic choriomeningitis virus. Also, Ben-Shahar *et al*. (1999) reported that the 26S proteasome alone could produce CTL epitopes of OVA efficiently, including $OVA_{257–264}$, and that the addition of PA28α/β had no enhancing effect. Our results indicate that PA28α/β is required for efficient presentation of some, but not all, antigens, and hence are generally in agreement with the observations made so far *in vitro*. What is unclear is whether PA28α/β is required for efficient processing of most antigens or only a restricted repertoire of antigens. We should be able to answer this question by testing many more different kinds of antigens in PA28α/β-deficient mice. It would also be interesting to ask what role PA28α/β might play in mice lacking LMP2 (Van Kaer *et al*., 1994) or LMP7 (Fehling *et al*., 1994). Under such suboptimal conditions, PA28α/β might play a more significant role in antigen presentation. Experiments are currently under way to test this possibility.

We previously made mice deficient in the PA28γ subunit (Murata *et al*., 1999). These mice did not display any obvious immunological abnormalities. However, whether PA28γ is involved in antigen presentation has not been fully addressed. In the present study, we tested the ability of PA28γ$^{-/-}$ and PA28α$^{-/-}$/β$^{-/-}$/γ$^{-/-}$ mice to process OVA proteins and TRP2 peptides (Figure 5). As expected from its known biological and biochemical properties, we failed to obtain any evidence for the involvement of PA28γ in antigen presentation. However, it will be necessary to examine more antigens, especially nuclear antigens, to draw a definite conclusion concerning the role of PA28γ in antigen presentation.

It is notable that proteasome-dependent proteolysis, as measured by antizyme-dependent ODC degradation, was attenuated moderately in PA28α$^{-/-}$/β$^{-/-}$ cell extracts, although the absence of PA28α/β did not affect the catalytic activities or specificities of the core 20S proteasome (Figure 3A–C). These results provide evidence that PA28α/β participates not only in ATP-independent short peptide hydrolysis, but also in ATP-dependent protein degradation. In the glycerol density gradient experiments (Figure 3B), PA28α$^{-/-}$/β$^{-/-}$ cell extracts displayed decreased ODC degradation activities around the 26S proteasome fractions compared with the wild-type extracts. This suggests that the decreased activities might have been caused by the lack of the hybrid proteasome, although the inability to separate hybrid proteasomes from 26S proteasomes by glycerol density gradient centrifugation precluded us from drawing a definitive conclusion.

Proteasomes are responsible for the elimination of proteins with abnormal conformations and of short-lived regulatory proteins. Hence, one can expect that many components of the proteasome are essential for survival. Indeed, analysis in yeast has shown that, with the exception of just one α-subunit, all components of the 20S proteasome are essential for cell viability (Tanaka, 1998). Since the PA28α/β-deficient mice were apparently healthy and had no obvious gross anatomical abnormalities, we can assume that the general housekeeping functions of proteasomes are not adversely affected by the absence of PA28α/β. Indeed, a pulse–chase experiment with splenocytes from wild-type and knockout mice revealed no obvious differences in the decay patterns of total cytosolic and membrane proteins (data not shown), indicating that PA28α/β does not influence the half-lives of most short-lived proteins. Thus, PA28α/β is likely to have a more specialized role in intracellular protein degradation *in vivo*. Recently, Takayanagi *et al*. (2000) demonstrated that osteoclastogenesis induced by RANKL [receptor activator of nuclear factor (NF)-κB ligand] was inhibited when co-stimulated with IFN-γ, and that this inhibition was caused by accelerated ubiquitin–proteasome-dependent proteolysis of TRAF6, an adaptor molecule essential for RANK/RANKL signal transduction. Interestingly, in the PA28α$^{-/-}$/β$^{-/-}$ mice, TRAF6 was not degraded upon co-stimulation with RANKL and IFN-γ, and accumulated in a ubiquitylated form, resulting in osteoclast formation. Thus, PA28α/β appears to influence the degradation of TRAF6. Although the precise underlying mechanism is still elusive, it seems likely that TRAF6 is degraded selectively by the hybrid proteasome containing PA28α/β. Such selective protein breakdown is consistent with our idea that PA28α/β plays an important role in the generation of class I ligands only for certain substrates. Therefore, it would be important to understand how PA28α/β confers unique substrate specificities upon the hybrid proteasome.

Materials and methods

Construction of the targeting vector

Mouse *PA28α* and *PA28β* genomic clones were isolated from a λ FIX II library made from the 129/SvJ strain as described before (Kohda *et al*., 1998). The targeting vector was constructed by cloning the following fragments into the pBluescript-SK vector in order of mention: a 5.8 kb *Apa*I–*Apa*I fragment from the 5′ end of the *PA28β* gene; a 1.2 kb *Xho*I–*Bam*HI fragment containing a neomycin-resistant gene (*Neo*) driven by the MC1 promoter for positive selection; a 6.5 kb *Cla*I–*Xba*I fragment from the intergenic region; a 2.2 kb *Ssp*I–*Ssp*I fragment from the 5′ end of the *PA28*α gene; and a 1.0 kb *Bgl*II–*Not*I fragment containing the diphtheria toxin gene (*DT-A*) derived from pMC1DT-3 for negative selection.

Gene targeting in ES cells and production of PA28α/β-deficient mice

The PA28α/β targeting construct was linearized with *Not*I and electroporated into TT2 ES cells. G418-resistant colonies were selected and isolated as described previously (Murata *et al*., 1999). Colonies of ES cells with homologous recombination events were identified by PCR using a 5′-primer (5′-TTTCCTGTACGTGACTTCCATCCTGTTG-3′) and a 3′-primer (5′-GGTCCACATACAATAAAGACATGGGCTG-3′). To verify the results of PCR screening, genomic DNA extracted from the PCR-positive ES clones was digested with *Bam*HI or *Eco*RV and hybridized with a probe (α-probe or β-probe in Figure 1A) derived from the 5′-flanking region of the *PA28α* or *PA28β* gene, respectively.

Germline transmission of the mutant allele was accomplished as described previously (Murata *et al*., 1999) and identified by Southern blot analysis. Progeny containing the mutant *PA28α/β* allele were intercrossed to obtain PA28α/β-deficient mice. Southern blot, northern blot and western blot analyses confirmed disruption of the *PA28α/β* genes.

PA28α/β/γ-deficient mice were generated by crossing PA28α/β-deficient mice with PA28γ-deficient mice (Murata *et al*., 1999).

Preparation of MEFs and cell culture

MEFs were obtained from day 13.5 embryos and cultured as previously described (Murata *et al*., 1999). IFN-γ (PeproTech) was used at 500 IU/ml when necessary.

Northern blot analysis

Northern blot analysis was performed as described previously (Murata *et al*., 1999). Total RNA was isolated from MEFs and various mouse tissues. Full-length mouse PA28α and PA28β cDNAs (Kandil *et al*., 1997) were labeled with ^{32}P using random primers and used as probes.

Tissue fractionation

Cytosolic and membrane proteins were fractionated by differential centrifugation of tissue homogenates. In brief, various tissues from mice were homogenized in isotonic buffer [25 mM Tris–HCl pH 7.5, 0.25 M sucrose, 1 mM dithiothreitol (DTT) and 1 mM phenylmethylsulfonyl fluoride (PMSF)] using a Potter–Elvehjem homogenizer. The resulting suspension was centrifuged at 10 000 *g* for 10 min. The supernatant was collected and centrifuged at 100 000 *g* for 1 h. The resulting pellet was dissolved in solubilizing buffer (25 mM Tris–HCl pH 7.5, 1% NP-40, 1 mM DTT, 1 mM PMSF) and used as a membrane fraction. The supernatant was used as a cytosolic fraction.

Western blot analysis

MEFs were lysed in lysis buffer (0.5% NP-40, 25 mM Tris–HCl pH 7.5, 1 mM DTT, 1 mM PMSF) and centrifuged at 15 000 *g* for 10 min (Figures 2 and 3D). The resultant supernatants were subjected to SDS–PAGE and blotted, and the blots were developed as described previously (Tanahashi *et al*., 2000). A 10 μg aliquot of total proteins was loaded onto each lane. In glycerol density gradient centrifugation experiments, 200 μl of every other fraction were precipitated with acetone and subjected to SDS–PAGE. The antibodies specific for PA28α, PA28β, PA28γ (Tanahashi *et al*., 1997), X, LMP2 (Hisamatsu *et al*., 1996) and Mss1 (Tanahashi *et al*., 1998) were described previously.

Sedimentation velocity analysis

MEFs and spleens were homogenized in a Potter–Elvehjem homogenizer in isotonic buffer containing 2 mM ATP. The homogenates were centrifuged at 15 000 *g* for 30 min. The supernatant was subjected to 10–40% glycerol density gradient centrifugation in 25 mM Tris–HCl buffer pH 7.5 containing 1 mM DTT and 2 mM ATP. After centrifugation at 83 000 *g* for 22 h in a Hitachi SRP28SA1 rotor, the gradient was separated into 30 fractions of 1 ml each.

Assay of peptidase activity

The hydrolysis of the synthetic peptides, succinyl-Leu-Leu-Val-Tyr-7-amino-4-methylcoumarin (Suc-LLVY-AMC), Boc-LRR-AMC and *N*-benzyloxycarbonyl-Leu-Leu-Glu-AMC (Cbz-LLE-AMC) was measured as described previously (Tanahashi *et al*., 1997). One unit of peptidase activity is defined as the amount degrading 1 nmol of given fluorogenic peptides per 1 min.

Assay of [^{35}S]ODC-degrading activity

The degradation of the recombinant ^{35}S-labeled ODC (2000–3000 c.p.m.) was assayed in the presence of ATP, an ATP-regenerating system and antizyme, as described before (Murakami *et al*., 1999). [^{35}S]ODC was produced by the *in vitro* translation system using rabbit reticulocyte lysates containing rat ODC mRNA, ^{35}S-labeled methionine and cysteine (NEN), and then purified by immunoaffinity chromatography prior to use. After incubation for 60 min at 37°C, the amount of trichloroacetic acid-soluble radioactivity of the reaction mixture was measured, and the activity was expressed as a percentage of total ODC added.

Two-dimensional gel electrophoresis

MEFs were cultured in the presence or absence of 500 IU/ml IFN-γ for 48 h. Then, MEFs were metabolically labeled with [^{35}S]methionine for 4 h followed by a 16 h chase. The MEFs were then lysed in lysis buffer (1% NP-40, 25 mM Tris–HCl pH 7.5, 150 mM NaCl, 1 mM DTT). Protein A–Sepharose beads pre-coated with anti-20S proteasome antibodies were incubated with pre-cleared lysates for 3 h at 4°C. Immunoprecipitates were solubilized in 8 M urea containing 2% NP-40 and 20 mM DTT, and subjected to isoelectric focusing using Immobiline DryStrip pH 3–10 and IPGphor (Amersham). After separation by SDS–PAGE, the gels were dried, exposed and developed with the BAS system (Fujifilm).

Virus and infection

The influenza virus strain A/Puerto Rico/8/34 (Flu PR8) was propagated in the allantoic cavity of 11-day-old embryonated chicken eggs. The allantoic fluid was titered by a plaque assay and stored in aliquots at –80°C until used. Female mice between 7 and 9 weeks of age were infected intranasally under diethyl ether anesthesia by depositing 30 μl of virus solution in phosphate-buffered saline (15 μl in each nostril). Blood was collected from the tail vein on days 0 and 12.

Antigen presentation assay

LPS blasts made from spleens were osmotically loaded with OVA proteins, $TRP2_{181–193}$ peptide (VYDFFVWLHYYSV) or $TRP2_{181–188}$ peptide (VYDFFVWL). Briefly, cells were suspended in 200 μl of warm (37°C) hypertonic buffer [0.5 M sucrose, 10% (w/v) polyethylene glycol 1000 in RPMI] with antigens, and incubated for 10 min at 37°C. Then, 15 ml of warm hypotonic buffer (RPMI1640/dH_2O: 60%) were added to this cell suspension and incubated for 2 min. After centrifugation, the cells were rinsed twice, incubated in plain RPMI for 3 h at 37°C in a humidified 5% CO_2 atmosphere and labeled with 3.7 MBq of $Na_2{}^{51}CrO_4$. The ^{51}Cr-labeled cells thus prepared were used as target cells to measure specific lysis by specific CTLs. The CTL assay was carried out in the presence of brefeldin A to block the egress of newly assembled MHC class I molecules from the endoplasmic reticulum to the cell surface. For negative control experiments, 50 μM lactacystin was added before and after antigen loading.

CTL induction from spleen cells

Spleen cells obtained from the wild-type and PA28$\alpha^{-/-}/\beta^{-/-}$ mice, which had survived the Flu PR8 infection, were incubated with 10 μM synthetic peptide $NS2_{114–121}$ (RTFSFQLI) or $NP_{366–374}$ (ASNENMETM) for 6 days. The cytolytic activities of primed splenocytes against EL-4 cells pulsed with each peptide were determined by the standard ^{51}Cr-release assay.

Acknowledgements

This work was supported in part by Grants-in-Aid for Scientific Research on Priority Areas (Intracellular Proteolysis) from The Ministry of Education, Culture, Sports, Science and Technology of Japan.

References

Ben-Shahar,S., Komlosh,A., Nadav,E., Shaked,I., Ziv,T., Admon,A., DeMartino,G.N. and Reiss,Y. (1999) 26S proteasome-mediated

production of an authentic major histocompatibility class I-restricted epitope from an intact protein substrate. *J. Biol. Chem.*, **274**, 21963–21972.

Bloom,M.B., Perry-Lalley,D., Robbins,P.F., Li,Y., El-Gamil,M., Rosenberg,S.A. and Yang,J.C. (1997) Identification of tyrosinase-related protein 2 as a tumor rejection antigen for the B16 melanoma. *J. Exp. Med.*, **185**, 453–459.

Bochtler,M., Ditzel,L., Groll,M., Hartmann,C. and Huber,R. (1999) The proteasome. *Annu. Rev. Biophys. Biomol. Struct.*, **28**, 295–317.

Brooks,P. *et al*. (2000) Subcellular localization of proteasomes and their regulatory complexes in mammalian cells. *Biochem. J.*, **346**, 155–161.

Coux,O., Tanaka,K. and Goldberg,A.L. (1996) Structure and functions of the 20S and 26S proteasomes. *Annu. Rev. Biochem.*, **65**, 801–847.

Dick,T.P., Ruppert,T., Groettrup,M., Kloetzel,P.M., Kuehn,L., Koszinowski,U.H., Stevanovic,S., Schild,H. and Rammensee,H.G. (1996) Coordinated dual cleavages induced by the proteasome regulator PA28 lead to dominant MHC ligands. *Cell*, **86**, 253–262.

Dubiel,W., Pratt,G., Ferrell,K. and Rechsteiner,M. (1992) Purification of an 11S regulator of the multicatalytic protease. *J. Biol. Chem.*, **267**, 22369–22377.

Fruh,K. and Yang,Y. (1999) Antigen presentation by MHC class I and its regulation by interferon γ. *Curr. Opin. Immunol.*, **11**, 76–81.

Fehling,H.J., Swat,W., Laplace,C., Kuhn,R., Rajewsky,K., Muller,U. and von Boehmer,H. (1994) MHC class I expression in mice lacking the proteasome subunit LMP-7. *Science*, **265**, 1234–1237.

Glickman,M.H., Rubin,D.M., Coux,O., Wefes,I., Pfeifer,G., Cjeka,Z., Baumeister,W., Fried,V.A. and Finley,D. (1998) A subcomplex of the proteasome regulatory particle required for ubiquitin-conjugate degradation and related to the COP9-signalosome and eIF3. *Cell*, **94**, 615–623.

Groettrup,M., Soza,A., Eggers,M., Kuehn,L., Dick,T.P., Schild,H., Rammensee,H.G., Koszinowski,U.H. and Kloetzel,P.M. (1996) A role for the proteasome regulator PA28α in antigen presentation. *Nature*, **381**, 166–168.

Hendil,K.B., Khan,S. and Tanaka,K. (1998) Simultaneous binding of PA28 and PA700 activators to 20S proteasomes. *Biochem. J.*, **332**, 749–754.

Hershko,A. and Ciechanover,A. (1998) The ubiquitin system. *Annu. Rev. Biochem.*, **67**, 425–479.

Hisamatsu,H. *et al*. (1996) Newly identified pair of proteasomal subunits regulated reciprocally by interferon γ. *J. Exp. Med.*, **183**, 1807–1816.

Kandil,E., Kohda,K., Ishibashi,T., Tanaka,K. and Kasahara,M. (1997) PA28 subunits of the mouse proteasome: primary structures and chromosomal localization of the genes. *Immunogenetics*, **46**, 337–344.

Kloetzel,P.M. (2001) Antigen processing by the proteasome. *Nature Rev. Mol. Cell. Biol.*, **2**, 179–87

Kohda,K., Ishibashi,T., Shimbara,N., Tanaka,K., Matsuda,Y. and Kasahara,M. (1998) Characterization of the mouse PA28 activator complex gene family: complete organizations of the three member genes and a physical map of the approximately 150-kb region containing the α- and β-subunit genes. *J. Immunol.*, **160**, 4923–4935.

Ma,C.P., Slaughter,C.A. and DeMartino,G.N. (1992) Identification, purification and characterization of a protein activator (PA28) of the 20S proteasome (macropain). *J. Biol. Chem.*, **267**, 10515–10523.

Murakami,Y., Matsufuji,S., Kameji,T., Hayashi,S., Igarashi,K., Tamura,T., Tanaka,K. and Ichihara,A. (1992) Ornithine decarboxylase is degraded by the 26S proteasome without ubiquitination. *Nature*, **360**, 597–599.

Murakami,Y., Matsufuji,S., Hayashi,S., Tanahashi,N. and Tanaka,K. (1999) ATP-dependent sequestration of ornithine decarboxylase by the 26S proteasome, a process coupled to unfolding, is a prerequisite for the degradation. *Mol. Cell. Biol.*, **19**, 7216–7227.

Murata,S., Kawahara,H., Tohma,S., Yamamoto,K., Kasahara,M., Nabeshima,Y., Tanaka,K. and Chiba,T. (1999) Growth retardation in mice lacking the proteasome activator PA28γ. *J. Biol. Chem.*, **274**, 38211–38215.

Niedermann,G., Geier,E., Lucchiari-Hartz,M., Hitziger,N., Ramsperger,A. and Eichmann,K. (1999) The specificity of proteasomes: impact on MHC class I processing and preparation of antigens. *Immunol. Rev.*, **172**, 29–48.

Noda,C., Tanahashi,N., Shimbara,N., Hendil,K.B. and Tanaka,K. (2000) Tissue distribution of constitutive proteasomes, immunoproteasomes and PA28 in rats. *Biochem. Biophys. Res. Commun.*, **277**, 348–354.

Preckel,T. *et al*. (1999) Impaired immunoproteasome assembly and immune responses in PA28$^{-/-}$ mice. *Science*, **286**, 2162–2165.

Rechsteiner,M., Realini,C. and Ustrell,V. (2000) The proteasome activator 11S REG (PA28) and class I antigen presentation. *Biochem. J.*, **345**, 1–15.

Reits,E.A., Vos,J.C., Gromme,M. and Neefjes,J. (2000) The major substrates for TAP *in vivo* are derived from newly synthesized proteins. *Nature*, **404**, 774–778.

Rock,K.L. and Goldberg,A.L. (1999) Degradation of cell proteins and the generation of MHC class I-presented peptides. *Annu. Rev. Immunol.*, **17**, 739–779.

Rock,K.L., Gramm,C., Rothstein,L., Clark,K., Stein,R., Dick,L., Hwang,D. and Goldberg,A.L. (1994) Inhibitors of the proteasome block the degradation of most cell proteins and the generation of peptides presented on MHC class I molecules. *Cell*, **78**, 761–771.

Schubert,U., Anton,L.C., Gibbs,J., Norbury,C.C., Yewdell,J.W. and Bennink,J.R. (2000) Rapid degradation of a large fraction of newly synthesized proteins by proteasomes. *Nature*, **404**, 770–774.

Schwarz,K., van den Broek,M., Kostka,S., Kraft,R., Soza,A., Schmidtke,G., Kloetzel,P.-M. and Groettrup,M. (2000a) Over-expression of the proteasome subunits LMP2, LMP7 and MECL-1, but not PA28α/β, enhances the presentation of an immunodominant lymphocytic choriomeningitis virus T cell epitope. *J. Immunol.*, **165**, 768–778.

Schwarz,K., Eggers,M., Soza,A., Koszinowski,U.H., Kloetzel,P.-M. and Groettrup,M. (2000b) The proteasome regulator PA28α/β can enhance antigen presentation without affecting 20S proteasome subunit composition. *Eur. J. Immunol.*, **30**, 3672–3679.

Stoltze,L., Nussbaum,A.K., Sijts,A., Emmerich,N.P., Kloetzel,P.M. and Schild,H. (2000) The function of the proteasome system in MHC class I antigen processing. *Immunol. Today*, **21**, 317–319.

Takayanagi,H. *et al*. (2000) T-cell-mediated regulation of osteoclasto-genesis by signalling cross-talk between RANKL and IFN-γ. *Nature*, **408**, 600–605.

Tanahashi,N. *et al*. (1997) Molecular properties of the proteasome activator PA28 family proteins and γ-interferon regulation. *Genes Cells*, **2**, 195–211.

Tanahashi,N., Fujiwara,T., Takahashi,E., Shimbara,N., Chung,C.H. and Tanaka,K. (1998) Chromosomal localization and immunological analysis of a family of human 26S proteasomal ATPases. *Biochem. Biophys. Res. Commun.*, **243**, 229–232.

Tanahashi,N., Murakami,Y., Minami,Y., Shimbara,N., Hendil,K.B. and Tanaka,K. (2000) Hybrid proteasomes: induction by interferon-γ and contribution to ATP-dependent proteolysis. *J. Biol. Chem.*, **275**, 14336–14345.

Tanaka,K. (1998) Molecular biology of the proteasome. *Biochem. Biophys. Res. Commun.*, **247**, 537–541.

Tanaka,K. and Kasahara,M. (1998) The MHC class I ligand-generating system: roles of immunoproteasomes and the interferon-γ-inducible proteasome activator PA28. *Immunol. Rev.*, **163**, 161–176.

Van Kaer,L., Ashton-Rickardt,P.G., Eichelberger,M., Gaczynska,M., Nagashima,K., Rock,K.L., Goldberg,A.L., Doherty,P.C. and Tonegawa,S. (1994) Altered peptidase and viral-specific T cell response in LMP2 mutant mice. *Immunity*, **1**, 533–541.

Voges,D., Zwickl,P. and Baumeister,W. (1999) The 26S proteasome: a molecular machine designed for controlled proteolysis. *Annu. Rev. Biochem.*, **68**, 1015–1068.

Wojcik,C. (1999) Proteasome activator subunit PA28α and related Ki antigen (PA28γ) are absent from the nuclear fraction purified by sucrose gradient centrifugation. *Int. J. Biochem. Cell Biol.*, **31**, 273–276.

Wojcik,C., Tanaka,K., Paweletz,N., Naab,U. and Wilk,S. (1998) Proteasome activator (PA28) subunits, α, β and γ (Ki antigen) in NT2 neuronal precursor cells and HeLa S3 cells. *Eur. J. Cell Biol.*, **77**, 151–160.

Yawata,M., Murata,S., Tanaka,K., Ishigatsubo,Y. and Kasahara,M. (2001) Nucleotide sequence analysis of the ~35-kb segment containing interferon-γ-inducible mouse proteasome activator genes. *Immunogenetics*, **53**, 119–129.

Zaiss,D.M. and Kloetzel,P.M. (1999) A second gene encoding the mouse proteasome activator PA28β subunit is part of a LINE1 element and is driven by a LINE1 promoter. *J. Mol. Biol.*, **287**, 829–835.

Received February 6, 2001; revised August 22, 2001; accepted September 13, 2001